

Akio Ohta  
Satoru Nakashima  
Hiroki Matsuyanagi  
Tsuyoshi Asakawa  
Shigeyoshi Miyagishi

## Krafft temperature and enthalpy of solution of *N*-acyl amino acid surfactants and their racemic modifications: effect of the counter ion

Received: 31 January 2003  
Revised: 18 April 2003  
Published online: 26 July 2003  
© Springer-Verlag 2003

A. Ohta (✉) · S. Nakashima  
H. Matsuyanagi · T. Asakawa  
S. Miyagishi  
Department of Chemistry and Chemical  
Engineering, Faculty of Engineering,  
Kanazawa University, 2-40-20 Kodatsuno,  
920-8667 Kanazawa, Ishikawa, Japan  
E-mail: akio-o@t.kanazawa-u.ac.jp  
Tel.: +81-76-234-4766  
Fax: +81-76-234-4800

**Abstract** The Krafft temperatures and enthalpies of solution of *N*-hexadecanoyl alaninate and valinate, and *N*-tetradecanoyl phenylalaninate were obtained from differential scanning calorimetry. The Krafft temperature of *N*-acyl amino acid surfactant increased with decreasing size of the counter ion, with some exceptions. The enthalpy of solution was endothermic and increased with decreasing size of the counter ion except for the cases of lithium salt. The results showed that the L-L interaction in the solid state of *N*-hexadecanoyl amino acid surfactant salt was superior to the D-L interaction for both the alanine and

valine systems when the counter ion size increased. However, the D-L interaction was still advantageous for the phenylalanine system with Cs<sup>+</sup> as a counter ion. Both Fourier transform infrared spectroscopy studies and theoretical calculations suggested that the difference in magnitudes of the interactions between peptide and counter ion was a dominant factor for the chiral effect.

**Keywords** *N*-Acyl amino acid surfactant · Krafft temperature · Enthalpy of solution · Counter ion · Chiral effect

### Introduction

*N*-Acyl amino acid surfactants are useful from both industrial and domestic viewpoints because of their biodegradability and low toxicity [1, 2]. However, concerns with their chiral discrimination has been growing since it has been reported that some amphiphiles containing peptide groups such as *N*-acyl amino acid were self-assembled to micrometer- and nanometer-scale structures [3, 4, 5, 6, 7]. It has been known that the chiral discrimination of *N*-acyl amino acid surfactants occurs remarkably in concentrated molecular organizations like solids [8, 9, 10], liquid crystal [11, 12], and condensed interfacial film [13, 14, 15, 16, 17]. In an earlier study [10], we showed by measurements of Krafft temperature (KT) and the enthalpy of solution of sodium *N*-hexadecanoyl amino acid surfactant salt that, in the solid

state, the heterochiral (D-L) interaction was superior to the homochiral one for both alanine (Ala) and phenylalanine (Phe) systems, while the homochiral (L-L or D-D) interaction was advantageous for both the valine (Val) and leucine systems. Further, we concluded that both peptide-peptide hydrogen bonding and steric hindrance of the amino acid residue govern the chiral effect. There are some studies on crystal structures of *N*-acyl amino acid in which hydrogen bonds between peptide-peptide groups and between peptide-carboxylic acid groups have been suggested [6, 18, 19, 20]. However, in the case of *N*-acyl amino acid salt, the interaction through the counter ion needs to be taken into account in addition to the hydrogen bond.

Therefore, in this study the effects of the counter ion size of *N*-acyl amino acid surfactants on the chiral discrimination were investigated through differential

scanning calorimetry (DSC) measurement of the KT and the enthalpy of solution. Additionally, we also studied their interaction in solid states by using Fourier transform infrared spectroscopy (FT-IR) measurements and theoretical calculations. FT-IR spectroscopy is one of the most powerful methods for analysis of the interactions of the peptide group of the *N*-acyl amino acid surfactant [21]. These are discussed from the viewpoint of interactions between peptide-peptide groups and between a peptide group and a counter ion.

## Materials and methods

**Materials** L-Ala, L-Val, L-Phe and their racemic mixtures (DL-form) were purchased from Peptide Institute and Nacalai Tesque, and used without further purification. *N*-Acyl amino acids (*Cn*-amino acid;  $n = 14, 16$ ) were synthesized by the reaction of an amino acid with hexadecanoyl or tetradecanoyl chlorides as described previously [22], and were re-crystallized from mixtures of either diethyl ether-ethanol or acetone-methanol. Their purities were checked by HPLC and DSC, and by observing no minimum on surface tension versus concentration curves at 298.15 K. *N*-Acyl amino acids were dissolved in 1 mM excess aqueous solution of alkali hydroxide (LiOH, NaOH, KOH, and CsOH) in order to prevent their precipitation.

**DSC analysis** DSC experiments were undertaken using a DSC7 (Perkin-Elmer) thermal analyzer. A sample solution was prepared by dissolving *N*-hexadecanoyl amino acids in an aqueous solution of 0.4 M chloride salt, which was sealed in a Large Volume Capsule (Perkin-Elmer) using an O-ring sealed 60  $\mu$ l stainless steel container. The addition of chloride salt was necessary in order to raise the KT above room temperature for almost all surfactants. The solutions were kept at 2 °C for a day to deposit the solid *N*-hexadecanoyl amino acid salts. The experiments were done using solutions in a concentration range of 10–20 mM using about 50 mg

of the samples. The samples were kept at 0 °C for 5 h, and then heated at a rate of 0.5 K/min. At least two runs were performed for each system.

**FT-IR analysis** Infrared absorption spectra were measured on a JASCO 460 Plus spectrometer by the KBr disc method. Salt samples were prepared by filtering the salts deposited from the alkali solutions of *N*-hexadecanoyl amino acid at 2 °C, and dried in vacuo at 40 °C for a day before measurement. Sixteen scans were accumulated at a resolution of 1  $\text{cm}^{-1}$ .

## Results and Discussion

### DSC analysis

The thermograms of 15 mM aqueous solution of *N*-hexadecanoyl alaninate and valinate surfactants in the presence of the solid deposit are shown in Fig. 1. It can be seen that an endothermic peak accompanies the dissolution of surfactants around the KT, which can be defined as the temperature corresponding to the onset of the peak; these values are shown in Table 1. It was confirmed that the KT values determined by this method are similar

**Table 1** Krafft temperatures of the surfactants

Counter ion	Krafft temperature K					
	C16-Ala		C16-Val		C14-Phe	
	L	DL	L	DL	L	DL
Li <sup>+</sup>	312.0	330.8	343.4	358.0	305.2	301.1
Na <sup>+</sup>	313.9	327.4	306.2	295.7	292.8	304.4
K <sup>+</sup>	309.2	302.5	-	-	290.3	298.4
Cs <sup>+</sup>	-	-	-	-	284.3	291.8

**Fig. 1** Thermograms of 15mM aqueous solutions of *N*-hexadecanoyl alaninate and valinate salts. Solid line L-form, dotted line DL-form

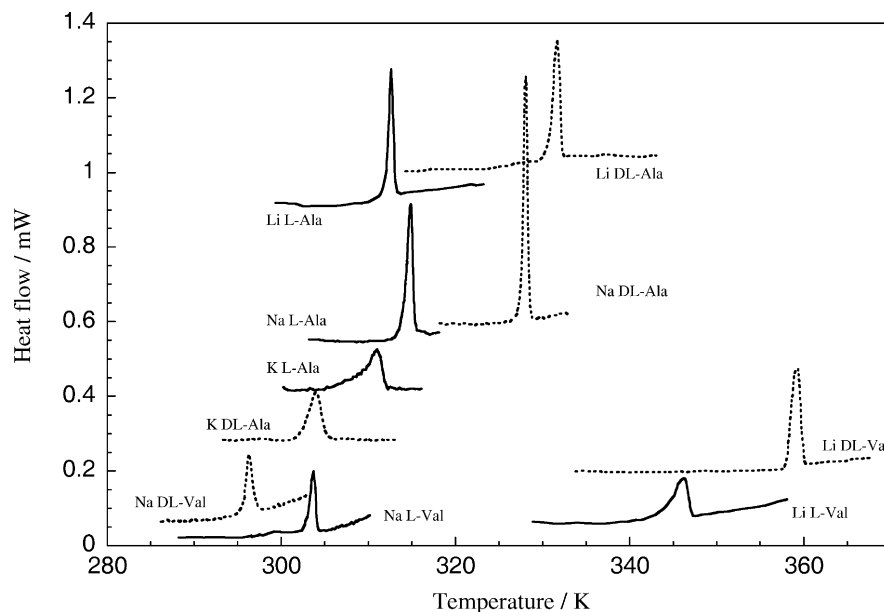
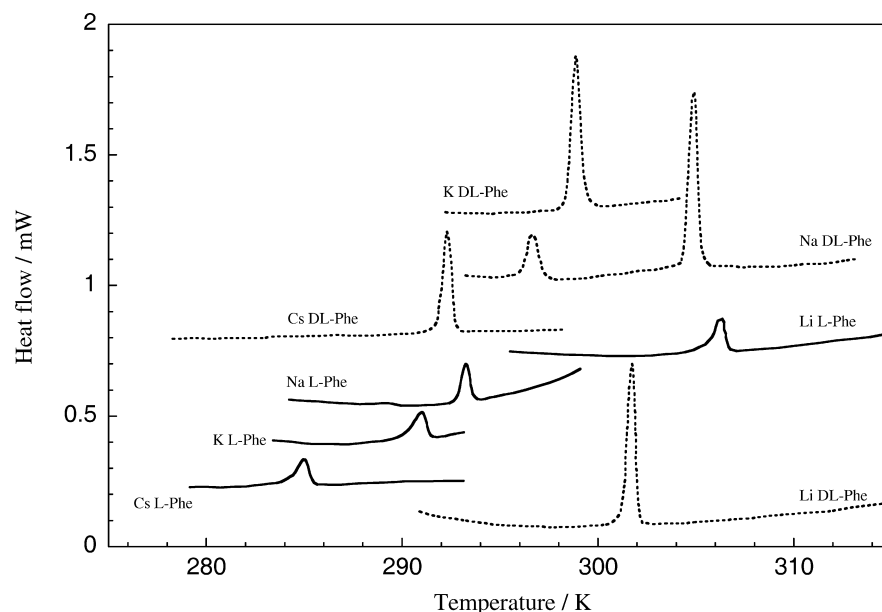


**Fig. 2** Thermograms of 15mM aqueous solutions of *N*-tetradecanoyl phenylalaninate salts. *Solid line* L-form, *dotted line* DL-form



to those obtained from the solubility measurements [10]. The thermograms of 15 mM aqueous solutions of *N*-tetradecanoyl phenylalaninate surfactants are shown in Fig. 2. The enthalpy of solution was calculated from the peak area and is shown in Table 2.

**Krafft temperature** It is seen that the KT of *N*-acyl amino acid surfactants increased with the decreasing size of the ion radius of counter ions except for the partial cases of the Li C16-L-Ala and Li C14-DL-Phe systems. This could be interpreted as the decrease in size of the counter ion making the molecular packing of the surfactant tighten, and the salting out effect enlarge. In particular, the gap of the KT value of C16-Val between Li and Na salts is surprisingly large, being more than 60 K in the case of C16-DL-Val. It is also seen that another peak appears at a lower temperature (269.2 K) than KT in the case of Na C14-DL-Phe; probably caused by a transition in the solid state. The transition enthalpy was 15.4 kJ mol<sup>-1</sup>.

The chiral effect of the amino acid can be divided into two types: first, where the KT of the DL-form is higher than that of the L-form, and second, where the opposite is the case. In the former, the heterochiral

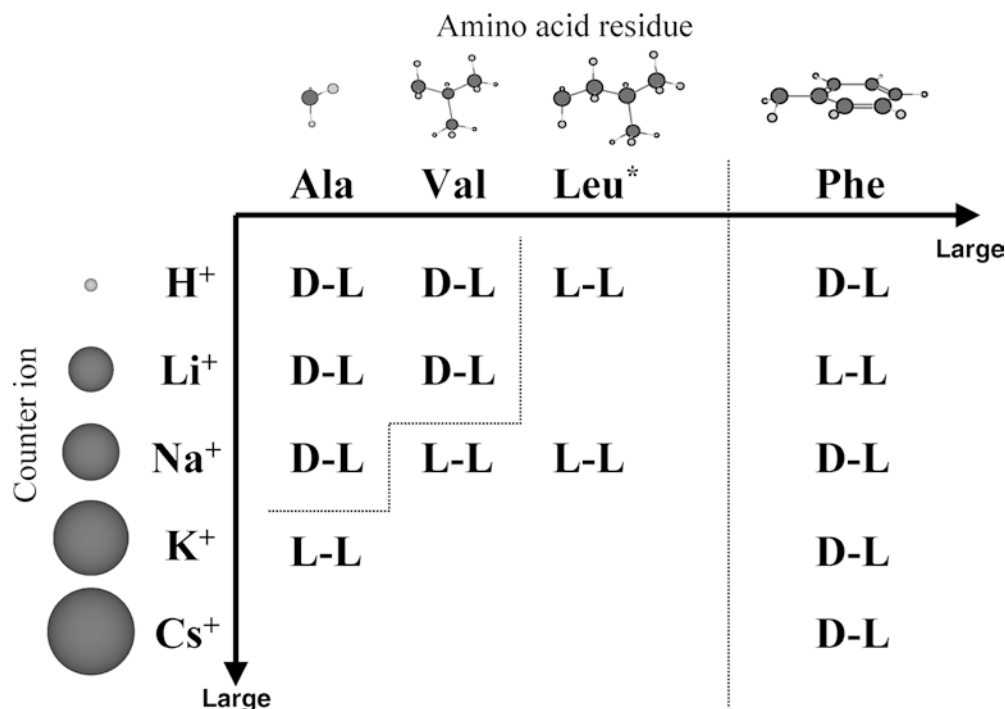
interaction is favored, while in the latter case the homochiral interaction is. An important point to emphasize is that the favorable interaction is shifted from heterochiral to homochiral with an increase in the counter ion radius for both C16-Ala and C16-Val. Figure 3 summarizes the trend in chiral interaction between the isomers of *N*-acyl amino acid surfactant with a higher KT in terms of both sizes of counter ions and the amino acid residue. Here, the case of H<sup>+</sup> as a counter ion was judged by the melting point of *N*-acyl amino acid [10]. This result suggests that the formation of a molecular pair between the L- and D-forms of the *N*-acyl amino acid surfactant is very effective in enhancing the molecular packing in the solid state, with decreasing size of the hydrophilic moiety. From the viewpoint of counter ion size as well as residue size, Phe, which contains an aromatic ring, can be considered an exceptional case. As mentioned in our earlier study [10], interactions between benzyl groups are favorable and are enhanced by a combination of the L- and D-forms. It is concluded that the heterochiral interaction in the *N*-acyl Phe system is extraordinarily strong, and remains favorable even when the counter ion is replaced by a large one such as Cs<sup>+</sup>. However, in

**Table 2** Enthalpies of solution of the surfactants

Counter ion	$\Delta h_{\text{sol}}$ kJ mol <sup>-1</sup>					
	C16-Ala		C16-Val		C14-Phe	
	L	DL	L	DL	L	DL
Li <sup>+</sup>	40.1 ± 4.1	52.2 ± 3.6	40.1 ± 2.1	56.4 ± 2.9	16.8 ± 1.5	50.0 ± 0.5
Na <sup>+</sup>	48.8 ± 2.1	61.8 ± 3.3	41.0 ± 1.5	38.1 ± 2.1	14.9 ± 1.1	61.9 ± 2.1 (15.4) <sup>a</sup>
K <sup>+</sup>	35.5 ± 3.8	36.2 ± 2.4	-	-	15.3 ± 0.8	55.9 ± 1.7
Cs <sup>+</sup>	-	-	-	-	14.9 ± 0.9	35.3 ± 1.9

<sup>a</sup>Transition enthalpy in solid state at 296.1 K

**Fig. 3** Schematic diagrams of the effects of the sizes of counter ions and of the amino acid residue on the chiral discrimination for the Krafft temperature (KT) of *N*-acyl amino acid salts [10]



the case of the Li C14-Phe system, the KT of the L-form was higher than that of the DL-form.

**Enthalpy of solution** The enthalpy of solution,  $\Delta h_{\text{sol}}$ , obtained in this study corresponds to the difference between the enthalpy of a surfactant in the micellar state  $h(\text{micelle})$  and that in the solid state  $h(\text{solid})$ .

$$\Delta h_{\text{sol}} = h(\text{micelle}) - h(\text{solid}) \quad (1)$$

There are two effects from the increase in size of the counter ion: one is the loosening of molecular packing in the solid state, and the other is the reduction of hydration of the counter ion in the micellar state. These effects raise the values of  $h(\text{solid})$  and  $h(\text{micelle})$ , respectively. From Table 2 we see that the  $\Delta h_{\text{sol}}$  value of the Na salt in C16-Ala systems is the largest, irrespective of chirality. Therefore, the difference in  $\Delta h_{\text{sol}}$  between Na and K salts is principally attributable to the value of  $h(\text{solid})$ , while that between Na and Li salts is caused by the variance of  $h(\text{micelle})$ . The  $\Delta h_{\text{sol}}$  value of C14-DL-Phe increases with decreasing counter ion size from Cs<sup>+</sup> to Na<sup>+</sup>. This is simply because the molecular packing in the solid state is tightened by the decrease in the counter ion size. In the C16-L-Val and C14-L-Phe systems, however, the  $\Delta h_{\text{sol}}$  value is not much affected by the size of the counter ion, and it is suggested that the counter ion size effect contributes equally to both  $h(\text{solid})$  and  $h(\text{micelle})$ .

Next, we examine the chiral effect of an amino acid on the enthalpy of solution. When the KT of the DL-form was higher than that of the L-form, the  $\Delta h_{\text{sol}}$  of

the DL-form was much larger than that of the L-form. Conversely for the case of Li C14-Phe, the  $\Delta h_{\text{sol}}$  value of the DL-form was much larger than that of the L-form, though the KT of the DL-form was lower than that of the L-form. On the other hand, for K C16-Ala and Na C16-Val systems, which are cases where the KT of the DL-form was lower than that of the L-form, there were no remarkable differences between the L- and DL-forms in the value of the  $\Delta h_{\text{sol}}$ . Since the racemic effect is very small in a micelle [22], the enthalpy of formation of a racemic compound  $\Delta h_{\text{rac}}$  could be evaluated by subtracting the  $\Delta h_{\text{sol}}$  value of the DL-form from that of the L-form, under the condition that the temperature dependence of enthalpy can be ignored.

$$\begin{aligned} \Delta h_{\text{rac}} &= h_{\text{DL}}(\text{solid}) - \frac{1}{2}[h_{\text{L}}(\text{solid}) + h_{\text{D}}(\text{solid})] \\ &= h_{\text{DL}}(\text{solid}) - h_{\text{L}}(\text{solid}) = \Delta h_{\text{sol,L}} - \Delta h_{\text{sol,DL}} \quad (2) \end{aligned}$$

The values obtained for  $\Delta h_{\text{rac}}$  of C16-Ala, Li C16-Val, and C14-Phe were ca.  $-13 \text{ kJ mol}^{-1}$ ,  $-16 \text{ kJ mol}^{-1}$ , and  $-20$  to  $-47 \text{ kJ mol}^{-1}$ , respectively. These values are much larger than the interaction energies between either methyl or benzyl groups, and correspond to a larger interaction energy, such as with hydrogen bonding or coordination. As mentioned in our previous study, it is quite likely that the combination of the L- and D-forms in those systems enhances the contribution of the coordination of carbonyl or carboxyl groups to alkali metal ions, as well as the contribution of hydrogen bonding between adjacent peptide groups [10]. This question is considered below. The  $\Delta h_{\text{rac}}$  value of Li C16-Ala is

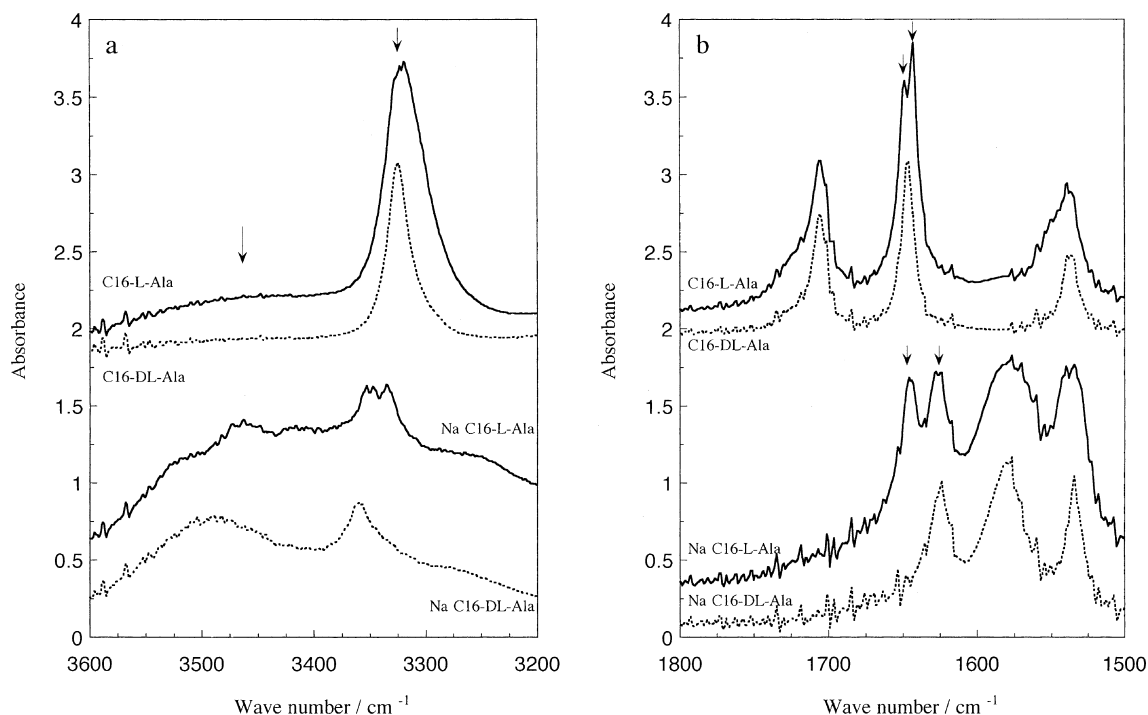


**Fig. 4a, b** FT-IR spectra of *N*-hexadecanoyl alanine and sodium *N*-hexadecanoyl alaninate. **a** 3,600–3,200  $\text{cm}^{-1}$ . **b** 1,800–1,500  $\text{cm}^{-1}$ . 1 C16-Ala(acid), 2 Na C16-Ala(salt), solid line L-form, dotted line DL-form

almost the same as that of Na C16-Ala, while the absolute value of  $\Delta h_{\text{rac}}$  of the C14-Phe system increases with decreasing counter ion size from  $\text{Cs}^+$  to  $\text{Na}^+$ . Judging from both the  $\Delta h_{\text{rac}}$  and the KT values of Li C14-Phe systems, the solid of Li C14-DL-Phe is a racemic compound and has much smaller entropy than that of Li C14-L-Phe.

### IR spectroscopy

Figure 4a shows FT-IR spectra of C16-Ala (acid) and Na C16-Ala (salt) in the solid state in the region of 3,600–3,200  $\text{cm}^{-1}$  where the key band is the N-H stretching vibration of the peptide group. Since the absorption band is shifted to a lower wave number by the hydrogen bonding, the bands around 3,500  $\text{cm}^{-1}$  and 3,340  $\text{cm}^{-1}$  are assigned the free and the hydrogen-bonded N-H stretching vibrations, respectively. From Fig. 4a it can be seen that the absorption of free N-H was absent for C16-DL-Ala, while the absorption for C16-L-Ala was just slightly detected. This supports the idea that the hydrogen bonding ability is a dominant factor for the difference in physicochemical properties between the L- and DL-forms of *N*-acyl amino acid. However, for Na-C16-Ala in Fig. 4a there is a rather large absorption of free N-H in both the L- and

DL-forms. Thus, it is difficult to explain the difference between the L- and DL-forms of Na-C16-Ala in terms of hydrogen bonding abilities. Figure 4b shows the same FT-IR spectra in the region of 1,800–1,500  $\text{cm}^{-1}$  where the key band is the C=O stretching vibration of the peptide or carboxyl groups. The absorption band around 1,705  $\text{cm}^{-1}$  is assigned the C=O stretching of the carboxyl group, and was shifted to around 1,580  $\text{cm}^{-1}$  by its neutralization to sodium carboxylate as shown in Fig. 4b. Without distinguishing between acid and salt systems, the absorption band of the DL-form resembles that of the L-form. However the absorption band of the C=O stretching vibration of the peptide group (amide I), which corresponds to the peak around 1,646  $\text{cm}^{-1}$ , precisely reflects the distinction of chirality. In the case of the acid form, there is a singlet peak for the DL-form in contrast to a doublet peak for the L-form. This corresponds to the result in Fig. 4a and suggests that the peptide group of C16-L-Ala has two states: one is a hydrogen-bonded state and another is a non-hydrogen-bonded state. On the other hand, in the case of Na L-Ala, a new absorption band appears at 1,625  $\text{cm}^{-1}$  in addition to the band around 1,646  $\text{cm}^{-1}$ . Furthermore the band around 1,646  $\text{cm}^{-1}$  is completely shifted to 1,623  $\text{cm}^{-1}$  in the case of Na DL-Ala. These bands appearing at the lower wave number could be assigned the C=O stretching vibration of the peptide group interacting with sodium ions. From these results it was determined that in the case of Na C16-DL-Ala, which has higher KT and  $h_{\text{sol}}$  values, the peptide group interacts with sodium ions more efficiently than in the case of Na C16-L-Ala.

From the above discussion, we can conclude that the observation of the C=O stretching vibration of the peptide group is the most advantageous way to examine the chiral effect of *N*-acyl amino acid salts. Figure 5 shows FT-IR spectra of other samples in the region of 1,800–1,500  $\text{cm}^{-1}$ . Interestingly, in the case of the K C16-Ala system, where the DL-form was less stable than the L-form, the band of the C=O stretching vibration of the peptide group of the DL-form only remained around 1,646  $\text{cm}^{-1}$ , in contrast to the case of Na C16-Ala (see Fig. 5a). However K C16-DL-Ala was a less-stable racemic compound, because the spectrum of K C16-DL-Ala was different to that of K C16-L-Ala. It can be seen from Fig. 5b that the spectrum of Na C16-DL-Val is almost the same as Na C16-L-Val; this suggests that Na C16-L-Val is not mixed or combined with Na C16-D-Val in the solid state. In Fig. 5b and c are results of Li C16-Val and K C14-Phe, where the DL-form is more stable than the L-form. It was found that the main band of the C=O stretching vibration of the peptide group of the DL-form appeared at a lower wavelength than that of the L-form in all systems. It might be concluded from these results that the difference in the interactions between the peptide group and the alkali metal ion governed chiral discrimination. However, for the Li C14-Phe system where the KT of the DL-form was lower than that of the L-form, the influence of chirality on the spectra was similar to that of the DL-form, which is more stable than the L-form. (see Fig. 5c) This result strongly supports the solid form of Li C14-DL-Phe being a racemic compound. The

reason that the KT of the DL-form of Li C14-Phe was lower than that of the L-form appears to be that the free energy of the DL-form is a higher value than the L-form owing to the smaller entropy.

### Theoretical calculation

In our earlier study [10], we applied *ab initio* calculations to the dimer of sodium *N*-acetyl alaninate (see Fig. 6a) as a model compound to simplify the calculations, and concluded that the difference in the magnitude of the peptide-peptide hydrogen bonding was the dominant factor for the chiral effect. From the FT-IR study, however, it is reasonable to suppose that the dominant factor is the difference in the coordination bonding between the peptide group and the alkali metal ion rather than that of the peptide-peptide hydrogen bonding. Therefore we must reconsider the obtained geometries from this standpoint. The optimized geometries were calculated using the restricted Hartree-Fock procedure with the 6-31+G\* basis set. All calculations were performed using Gaussian 98 [23].

The top views of obtained geometries of the L-L and D-L dimers are shown in Fig. 6b. The top views of the two structures seem to be similar, however, the difference is clear from the side view of them in Fig. 6c. In the D-L dimer, each Ala residue is situated in the *trans* position through the bonding between carboxylates, while it is in the *gauche* position for the L-L dimer. Furthermore, it was found that the dimers could interact with the two adjacent molecules at the two coordination bond lines. It should also be noted that one line is parallel to the other in the D-L dimer, whereas the two lines

**Fig. 5a–c** Fourier transform-IR spectra of *N*-acyl amino acid salts. **a** C16-Ala. **b** C16-Val. **c** C14-Phe. Solid line L-form, dotted line DL-form

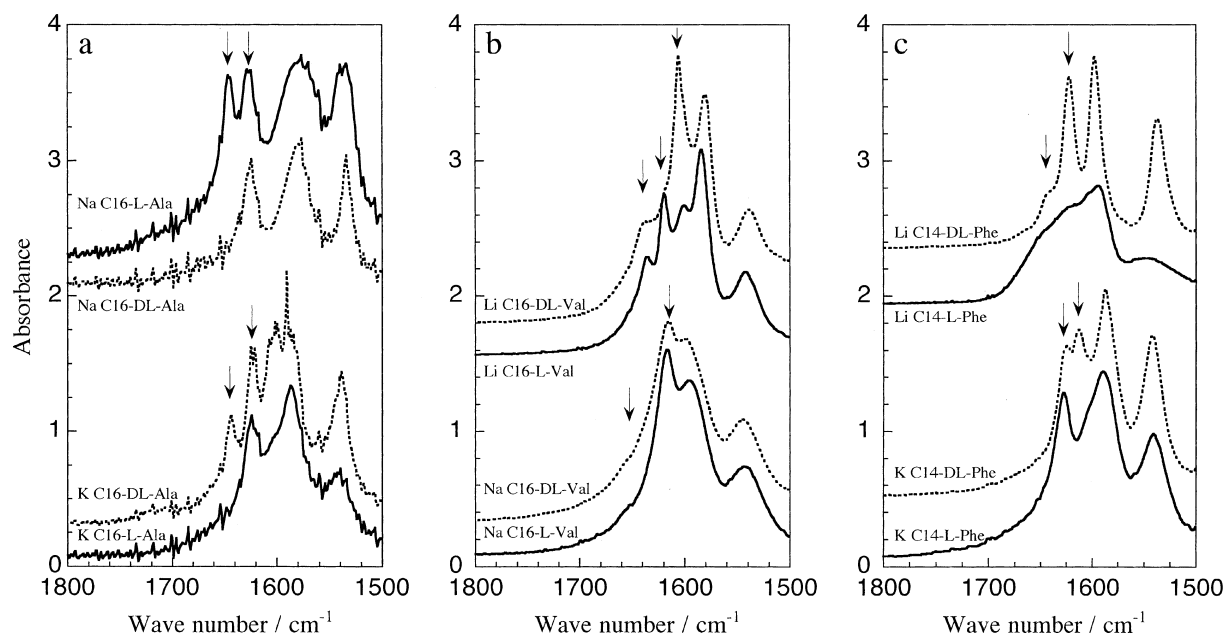


**Fig. 6** **a** Chemical structure of dimer of sodium *N*-acetyl alaninate. **b** Top view of optimized dimer geometries. **c** Side view of optimized dimer geometries

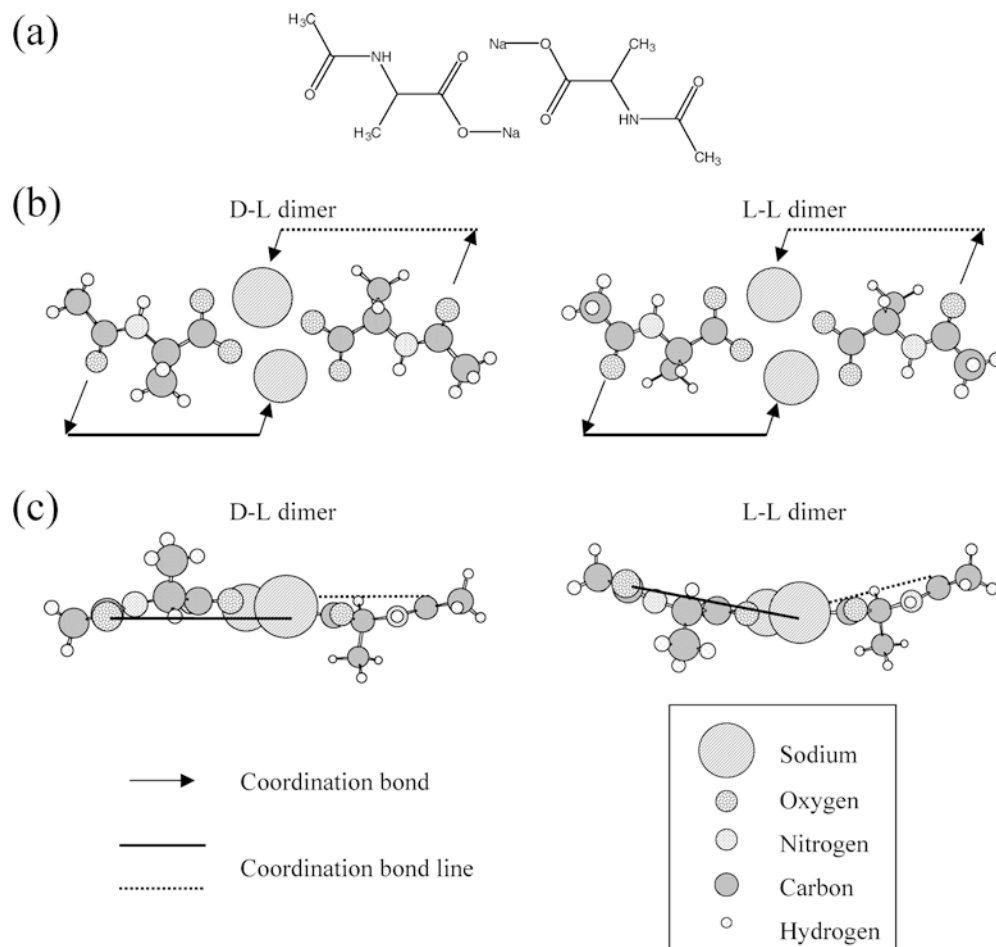
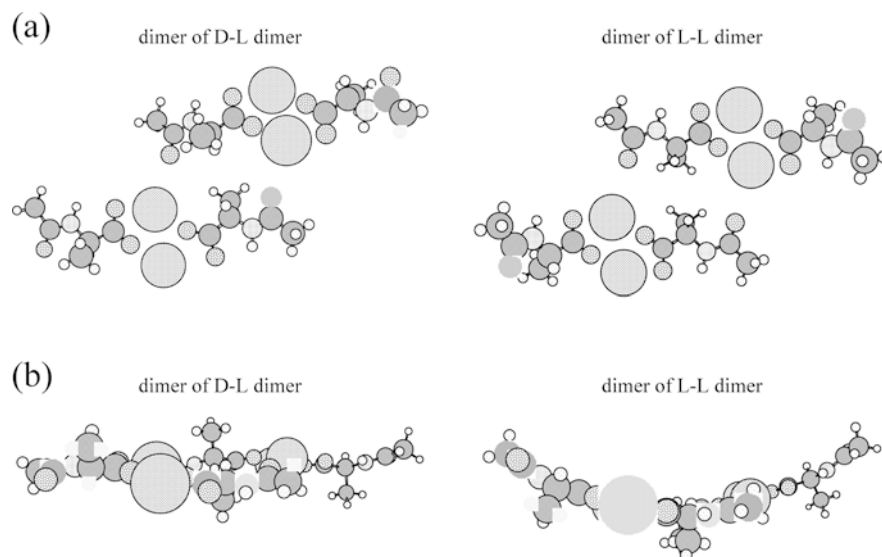


**Fig. 7** **a** Top views of optimized geometries of dimer of dimer of sodium *N*-acetyl alaninate. **b** Side views of optimized geometries



intersect each other in the L-L dimer (Fig. 6c). This suggests that the DL form of Na *N*-acetyl alaninate can create a sheet structure stabilized by interaction between

the peptide group and the sodium ion more effectively than can the L-form. To further substantiate this assumption, semi-empirical MO calculations were

applied to the dimer of the dimer obtained by the *ab initio* calculations. These calculations were performed using MOPAC 2000 with PM3 Hamiltonian [24] under the condition that the geometries of dimers by *ab initio* calculation were fixed. Obtained geometries of the dimer of the DL- and LL-dimers are shown in Fig. 7: it can be seen that the C=O group of peptides did not interact with the N-H group of peptides, but with sodium ions in both cases. Furthermore the axes of the two dimers intersected each other in the case of the LL-dimer, while, as expected, there were two dimers on an almost identical plane in the case of the DL-dimer. Therefore, Na *N*-acyl DL-alaninate becomes a racemic compound in the solid state. This could explain why Na *N*-acyl DL-valinate and K *N*-acyl DL-alaninate are less stable than their L-form counterparts, since the larger hydrophobic residues and counter ions may hinder stacking in the sheet-like structures. Conversely, in the case of Na *N*-acyl DL-phenylalaninate, contact between the benzyl

groups in the sheet structure is an advantageous factor and results in the racemic compound.

In summary, the Krafft temperature of *N*-acyl amino acid surfactant increased with decreasing size of the counter ion, except for the cases of Li C16-L-Ala and Li C14-DL-Phe. Experimental results showed that the L-L interaction became superior to the D-L interaction in the solid state of *N*-acyl amino acid surfactant salt for the Ala and Val systems when the size of the counter ion size increased, while the D-L interaction was still advantageous for the Phe system if the counter ion was replaced by a large one such as Cs<sup>+</sup>. It was suggested that both interaction between the peptide and the counter ion, and steric hindrance of the amino acid residue govern the chiral effect.

**Acknowledgement** This research was supported by the Sasakawa Scientific Research Grant from Japan Science Society and Mukai Science and Technology Foundation.

## References

1. Takehara M (1984) Hyomen (in Japanese) 35:459
2. Takehara M (1984) Colloids Surf 38:149
3. Kogiso M, Ohnishi S, Yase K, Masuda M, Shimizu T (1998) Langmuir 14:4978
4. Matsui H, Gologan B (2000) J Phys Chem B 104:3383
5. Ariga K, Kikuchi J, Naito M, Koyama E, Yamada N (2000) Langmuir 16:4929
6. Schneider J, Messerschmidt C, Schulz A, Gnade M, Schade B, Luger P, Bombicz P, Hubert V, Fuhrhop JH (2000) Langmuir 16:8575
7. Matsui H, Douberly Jr GE (2001) Langmuir 17:7918
8. Miyagishi S, Matsumura S, Murata K, Asakawa T, Nishida M (1985) Bull Chem Soc Jpn 58:1019
9. Miyagishi S, Matsumura S, Asakawa T, Nishida M (1986) Bull Chem Soc Jpn 59:557
10. Ohta A, Ozawa N, Nakashima S, Asakawa T, Miyagishi S (2003) Colloid Polym Sci 281–363
11. Sakamoto K, Hatano M (1980) Bull Chem Soc Jpn 53:339
12. Sakamoto K (1980) Mol Cryst Liq Cryst 59:59
13. Harvry NG, Mirajovsky D, Rose PL, Verbiar R, Arnett RM (1989) J Am Chem Soc 111:1115
14. Stine KJ, Uang JY-J, Dingman SD (1993) Langmuir 9:2112
15. Gericke A, Hühnerfuss H (1994) Langmuir 10:3782
16. Parazak DP, Uang J Y-J, Turner B, Stine KJ (1994) Langmuir 10:3787
17. Hoffmann F, Hühnerfuss H, Stine KJ (1998) Langmuir 14:4525
18. Donohue J, Marsh RE (1962) Acta Cryst 15:941
19. Cole FE (1970) Acta Cryst B26:622
20. Lovas G, Kalman A, Argay G (1974) Acta Cryst B30:2882
21. Du X, Liang Y (2000) Langmuir 16:3422
22. Miyagishi S, Nishida M (1978) J Colloid Interface Sci 65:380
23. Frisch MJ, Trucks GW, Schlegel HB, Scuseria GE, Robb MA, Cheeseman JR, Zakrzewski VG, Montgomery JA, Stratmann RE, Burant JC, Dapprich S, Millam JM, Daniels AD, Kudin KN, Strain MC, Farkas O, Tomasi J, Barone V, Cossi M, Cammi R, Mennucci B, Pomelli C, Adamo C, Clifford S, Ochterski J, Petersson GA, Ayala PY, Cui Q, Morokuma K, Malick DK, Rabuck AD, Raghavachari K, Foresman JB, Cioslowski J, Ortiz JV, Stefanov BB, Liu G, Liashenko A, Piskorz P, Komaromi I, Gomperts R, Martin RL, Fox DJ, Keith T, Al-laham MA, Peng CY, Nanayakkara A, Gonzalez C, Challacombe M, Gill PMW, Johnson BG, Chen W, Wong MW, Andres JL, Head-Gordon M, Replogle ES, Pople JA (1998) Gaussian 98 (Revision A.9). Gaussian, Pittsburgh, Pa.
24. Stewart JJP (1989) J Comp Chem 10:209